



UNIVERSITY OF LEEDS

This is a repository copy of *A high-throughput multi-microfluidic crystal generator (MMicroCryGen) platform for facile screening of polymorphism and crystal morphology for pharmaceutical compounds.*

White Rose Research Online URL for this paper:  
<http://eprints.whiterose.ac.uk/132315/>

Version: Accepted Version

---

**Article:**

Simone, E [orcid.org/0000-0003-4000-2222](https://orcid.org/0000-0003-4000-2222), McVeigh, J, Reis, NM et al. (1 more author) (2018) A high-throughput multi-microfluidic crystal generator (MMicroCryGen) platform for facile screening of polymorphism and crystal morphology for pharmaceutical compounds. *Lab on a Chip* (15). pp. 2235-2245. ISSN 1473-0197

<https://doi.org/10.1039/c8lc00301g>

---

This is an author produced version of a paper published in *Lab on a Chip*. Uploaded in accordance with the publisher's self-archiving policy.

**Reuse**

Items deposited in White Rose Research Online are protected by copyright, with all rights reserved unless indicated otherwise. They may be downloaded and/or printed for private study, or other acts as permitted by national copyright laws. The publisher or other rights holders may allow further reproduction and re-use of the full text version. This is indicated by the licence information on the White Rose Research Online record for the item.

**Takedown**

If you consider content in White Rose Research Online to be in breach of UK law, please notify us by emailing [eprints@whiterose.ac.uk](mailto:eprints@whiterose.ac.uk) including the URL of the record and the reason for the withdrawal request.



[eprints@whiterose.ac.uk](mailto:eprints@whiterose.ac.uk)  
<https://eprints.whiterose.ac.uk/>

# Lab on a Chip

Accepted Manuscript



This article can be cited before page numbers have been issued, to do this please use: E. Simone, J. McVeigh, N. M. Reis and Z. Nagy, *Lab Chip*, 2018, DOI: 10.1039/C8LC00301G.



This is an Accepted Manuscript, which has been through the Royal Society of Chemistry peer review process and has been accepted for publication.

Accepted Manuscripts are published online shortly after acceptance, before technical editing, formatting and proof reading. Using this free service, authors can make their results available to the community, in citable form, before we publish the edited article. We will replace this Accepted Manuscript with the edited and formatted Advance Article as soon as it is available.

You can find more information about Accepted Manuscripts in the [author guidelines](#).

Please note that technical editing may introduce minor changes to the text and/or graphics, which may alter content. The journal's standard [Terms & Conditions](#) and the ethical guidelines, outlined in our [author and reviewer resource centre](#), still apply. In no event shall the Royal Society of Chemistry be held responsible for any errors or omissions in this Accepted Manuscript or any consequences arising from the use of any information it contains.

1 **A high-throughput multi-microfluidic crystal generator (MMicroCryGen)**  
2 **platform for facile screening of polymorphism and crystals morphology for**  
3 **pharmaceutical compounds**

4 E. Simone<sup>\*,a,b</sup>, J. McVeigh<sup>b</sup>, N.M. Reis<sup>b,c</sup>, Z.K. Nagy<sup>b,d</sup>

5 <sup>a</sup> *School of Food Science and Nutrition, University of Leeds, Leeds, LS2 9JT, UK. E-mail:*

6 *[e.simone@leeds.ac.uk](mailto:e.simone@leeds.ac.uk); Tel: +44(0)113 343 1424*

7 <sup>b</sup> *Department of Chemical Engineering, Loughborough University, Loughborough, LE11 3TU, UK*

8 <sup>c</sup> *Department of Chemical Engineering, University of Bath, Bath, BA2 7AY, UK. E-mail:*

9 *[n.m.reis@bath.ac.uk](mailto:n.m.reis@bath.ac.uk); Tel: +44 (0)1225 383 369*

10 <sup>d</sup> *Davidson School of Chemical Engineering, Purdue University, West Lafayette, IN 47907-2100, USA.*

11 *E-mail: [z.k.nagy@lboro.ac.uk](mailto:z.k.nagy@lboro.ac.uk); [zknagy@purdue.edu](mailto:zknagy@purdue.edu); Tel: +1 (765) 494-0734*

12 *\* Corresponding author*

13

14 **Keywords:** polymorph screening, single crystal generator, 'dip stick' microfluidics,  
15 crystallization.

16

17 **Abstract**

18 In this work a novel multi-microfluidic crystallization platform called MMicroCryGen is  
19 presented, offering a facile methodology for generating individual crystals for fast and easy  
20 screening for polymorphism and crystal habit of solid compounds. The MMicroCryGen  
21 device is capable of performing 8×10 cooling crystallization experiments in parallel using 8  
22 disposable microcapillary film strips, each requiring less than 25 µL of solution. Compared to  
23 traditional microfluidic systems the MMicroCryGen platform does not require complex fluid

24 handling, it can be directly integrated with a 96 wells microplate and it can also work in  
25 “dipstick” mode. The produced crystals can be safely and directly observed inside the  
26 capillaries with optical and spectroscopic techniques. The platform was validated by  
27 performing a number of independent experimental runs for: (1) polymorph and hydrate  
28 screening for ortho-aminobenzoic acid, succinic acid and piroxicam; (2) co-crystal form  
29 screening for the p-Toluenesulfonamide/triphenylphosphine oxide system; (3) studying the  
30 effect of o-toluic acid on ortho-aminobenzoic cooling crystallization (effect of structurally  
31 related additives). In all three cases, all known solid forms were identified with a single  
32 experiment using ~200  $\mu$ L of solvent and just few micrograms of solid material. The  
33 MMicroCryGen is simple to use, inexpensive and it provides increased flexibility compared  
34 to traditional crystallization techniques, being an effective new microfluidic solution for solid  
35 form screening for pharmaceutical, fine chemicals, food and agrochemical industries.

36

## 37 **Introduction**

38 Polymorphism is known as the ability of a compound to exist in more than one crystalline  
39 structure and is very common in the crystallization of active pharmaceutical ingredients  
40 (APIs) (1). Polymorph screening is therefore essential during the development of new drugs  
41 since the formation of the wrong polymorph can affect solubility, rate of dissolution and  
42 toxicity of the API (1-3). The discovery of possible polymorphic forms for newly synthesized  
43 compounds is usually done by running independent crystallization experiments in small,  
44 bench scale (1-100 mL) crystallizers or via high-throughput devices based on arrays of wells,  
45 tubes or vials. This task requires a large number of steps and it is often difficult and  
46 expensive to automate because of the complex fluid handling involved (4, 5). Robotic liquid  
47 handling systems provided the mean to automate and increase throughput for screening of  
48 novel compounds in a drug discovery environment (6); however, the high cost of such  
49 systems means the technology is only accessible to few.

50 In recent years microfluidic devices have been used to study several crystallization steps,  
51 including nucleation and growth (7-11), polymorphism (12-14) and co-crystal formation (15).  
52 Microfluidic technologies offer the possibility of running several experiments in parallel  
53 using small quantities of API, which is particularly important during the early stages of  
54 clinical trials when only small quantity of API is available. Nevertheless, current microfluidic  
55 devices still require interface to complex fluid handling (16). Furthermore, the extraction of  
56 crystals from the microfluidic channels for off-line analysis can also be problematic.

57 Droplet-based devices are the most commonly used microfluidic tools for measuring  
58 nucleation rate, metastable zone width as well as solubility, and for the screening of  
59 polymorphs (7, 16-21). The main advantage of using droplets for crystal formation is that a  
60 small volume of solution can be isolated in an easy way such as using a manual or electronic  
61 pipette (20), or by segmenting the solution flow with an immiscible liquid or gas in a

62 microchannel (17-19). The supersaturation necessary to form crystals can then be generated  
63 by decrease the temperature of the droplets (7), adding an anti-solvent or a reactant (19) or  
64 via solvent evaporation (20). Each droplet can be considered as a single crystallizer allowing  
65 a systematic determination of the primary nucleation kinetic as well as an easier  
66 determination of the polymorphism of each crystal nucleated. Furthermore, the wells  
67 containing the droplets for evaporation-based devices can be chemically functionalized via  
68 self-assembled monolayers of specific organic compounds. In this way polymorphism can be  
69 controlled via templated heterogeneous nucleation (20, 21). Despite these advantages, the  
70 droplet-based devices that use micro-channels to mix immiscible liquids require the use of  
71 external pumps, precise flow control for the mixing of the two immiscible phases and  
72 complex microchannel geometry. Additionally, in the case of evaporation-based  
73 microfluidics, a controlled atmosphere around the droplets is necessary for a slow and  
74 controlled removal of the solvent.

75 Both cooling and anti-solvent crystallization processes have been conducted in microfluidic  
76 channels with precise control of both temperature and solute concentration (12). Because of  
77 the reduced amount of crystallizing material needed, microfluidic devices are particularly  
78 convenient for the study of expensive compounds such as proteins (22, 23), or for safe  
79 handling of toxic and/or carcinogenic compounds (16). Compared to larger scale  
80 crystallizers, microfluidic crystallizers provide a micro-environment with laminar only  
81 mixing conditions that enable the formation of high quality crystals, with defined habit and  
82 limited structural defects or amorphicity. Such crystals can easily be analysed via optical  
83 microscopy, vibrational spectroscopy and, in some cases X-ray diffraction (16). Microfluidic  
84 devices are also particularly suited for polymorph screening. In fact, the reduced volume and  
85 the absence of turbulent mixing promotes primary over secondary nucleation and favours the  
86 discovery of a larger number of polymorphs and co-crystals (13-16). Furthermore, in small

87 volumes the nucleation and persistence of highly unstable polymorphs is more likely  
88 compared to large scale crystallizers (12-14, 16, 24). It is worth noticing that the rate of  
89 nucleation in small volumes is always slower than for large crystallizers, and the formation of  
90 crystals that are large enough to be analysed takes a longer time.

91 Despite the evident advantages of microfluidics technologies, current devices remain  
92 expensive to produce at small scale, require bulky fluid handling equipment and present  
93 solvent-compatibility issues.

94 In this work a novel multi-microfluidic platform for the generation of individual separated  
95 crystals (MMicroCryGen) that allows rapid and facile screening for polymorphism and  
96 crystal habit from a small sample volume is presented for the first time. In contrast to existent  
97 droplet-based microfluidic devices for polymorph screening (17-20) the MMicroCryGen does  
98 not require external pumps as sample is loaded by capillary action (similar to a conventional  
99 ‘dipstick’ test) and crystals are generated by cooling, with smoother control of the  
100 supersaturation during nucleation.

101 The MMicroCryGen device shown in Figure 1a was specifically designed to perform  
102 multiple cooling crystallization experiments in parallel, with the option of real-time, *in-situ*  
103 observation of the crystals using optical or spectroscopic sensors. This platform can be used  
104 for the screening of hydrates, salts and co-crystals, which are often used as expedients to  
105 improve the rate of dissolution and solubility of an API, as well as to study the morphology  
106 of the crystals in different solvents.

107 The main consumable of the MMicroCryGen is a set of multiplex, microfluidic strips  
108 obtained via cutting a longer MicroCapillary Film (MCF). The MCF is a flat film containing  
109 an array of ten parallel microcapillaries fabricated from fluorinated ethylene propylene co-  
110 polymer (Teflon-FEP®) using a novel continuous melt-extrusion process (25, 26). Photos of

111 the MCF strips are shown in Figure 1b and c. Due to the geometry and optical properties of  
112 FEP-Teflon®, the microcapillaries are uniquely transparent in a very broad range of  
113 wavelengths including UV, VIS and NIR. Additionally, the MCF material is available in  
114 different inner internal diameters as reported elsewhere (27). Although FEP-Teflon® is  
115 naturally hydrophobic, internal coating of the microcapillaries with a hydrophilic hydrogel  
116 (28) enables the aspiration of fluid sample from a conventional microtiter plate by capillary  
117 action. Small volumes of API solutions (around 25  $\mu$ L) can be prepared and aspirated into the  
118 microcapillaries without the use of pumps or syringes, similarly to conventional ‘dip stick’  
119 tests. The small volume, low cost, transparency and hydrophilicity of the MCF material  
120 makes it an optimal consumable capillary element for the MMicroCryGen platform. The  
121 device uses a Peltier heat exchanger for carrying out controlled cooling crystallizations,  
122 enabling the study of both crystal morphology and polymorphism. In this work, the  
123 MMicroCryGen platform was validated by carrying out polymorph screening of succinic acid  
124 (SA) and ortho-aminobenzoic acid (OABA) (29-32), by determining the effect of o-toluic  
125 acid (OTA) on the polymorphism of OABA and by studying the formation of hydrates of  
126 piroxicam and co-crystals of p-Toluenesulfonamide (p-TSA) and Triphenylphosphine oxide  
127 (TPPO) (33). The data presented show that the MMicroCryGen is a valuable microfluidic  
128 solution for facile polymorph screening of APIs since it requires a smaller amount of drugs  
129 and solvents and considerably less and cheaper additional instrumentation compared to  
130 standard techniques. The device can be particularly useful during the early stages of drug  
131 development when only a small amount of material is available and for the study of toxic,  
132 genotoxic or carcinogenic APIs.

133

134 **Experimental**



### 135 **Materials**

136 For the screening experiments succinic acid (SA, from Sigma Aldrich,  $\geq 99.0$  % purity),  
137 ortho-aminobenzoic acid (OABA, from Sigma Aldrich, purity  $>98\%$ ), piroxicam (from  
138 Hangzhou Hyper Chemicals Limited, 99 % purity, anhydrous), o-toluic acid, (OTA, from  
139 Sigma Aldrich, 99% purity) and p-Toluenesulfonamide (p-TSA, 99 %) and  
140 triphenylphosphine oxide (TPPO, 99 %) was sourced from Sigma-Aldrich (Dorset, UK) and  
141 used as received. Deionized water (Millipore ultrapure water system) isopropyl alcohol (IPA  
142 99.97 % grade, Fisher Scientific, Loughborough, UK), acetone (Fisher Scientific,  $>99.98$  %  
143 grade) and acetonitrile (Fisher Scientific, grade 99.9 %) were used as solvents.

### 144 **Multi-Microfluidic Crystal Generator (MMicroCryGen)**

145 Figure 2 shows the miniaturised MMicroCryGen device, developed and built in house at  
146 Loughborough University (UK). The main element is a re-usable frame (60.0 mm $\times$ 78.8 mm,  
147 as shown in the drawings provided in the Supporting Information) composed of an  
148 aluminium plate, a central transparent Perspex cover and two side aluminium edges used for  
149 sealing the MCF strips and keeping them in a flat position (Figure 2a and 2d). The frame has  
150 8 slots for the insertions of 70-80 mm long MCF strips. The slots are spaced by 8.36 mm  
151 centre-to-centre, enabling the direct interface with a 96 wells microplate (Figure 2d). Each  
152 MCF strip has an internal volume of approximately 25  $\mu\text{L}$  and each 2.5  $\mu\text{L}$  microcapillary  
153 can be considered as a single crystallizer with no mixing. Although the MMicroCryGen was  
154 operated manually, it offers the opportunity for easy automation with a robot arm, and does  
155 not require any fluid handling equipment/pumps. The MCF strips are kept in a flat position  
156 on the plate and sealed at both ends to avoid solvent evaporation by compressing the central  
157 Perspex cover and the two lateral aluminium edges with three sets of four screws. The lateral  
158 edges are provided with 8 pointy protrusions that compress both edges of the MCF strips.  
159 Although in this work the whole frame was kept in position using three sets of screws (Figure

160 2b), the design could be further simplified with a one-step, 'clip' mechanism. The capillaries  
161 could be observed in real time through the Perspex cover using optical or spectroscopic  
162 sensors.

163 The whole aluminium frame containing the MCF strips lay on a polyoxymethylene plate that  
164 contains a Peltier unit for temperature control (Meerstetter Engineering TEC-1090, Rubigen,  
165 Switzerland, shown in Figure 2b). The Peltier element (ThermaTEC™ Series HT4, Laird  
166 Technologies, London United Kingdom) allows a range of temperatures in the  
167 microcapillaries between -20 and 120 °C and a maximum cooling rate of 5 °C/min. The  
168 Peltier unit is connected to a fan (BIG Shuriken 2, model SCBSK-2100 purchased from  
169 Scythe, Tokyo, Japan) and a controller (Meerstetter Engineering TEC-1091 running with  
170 TEC Service v3.0) for temperature regulation. Multiple units could be arranged in parallel  
171 and controlled independently for a higher number of simultaneous experiments.

172

173

#### 174 ***Fabrication of hydrophilic microfluidic, MCF strips***

175 The MCF material was manufactured by Lamina Dielectrics Ltd (Billingshurst, West Sussex,  
176 UK) from Teflon® FEP (Dupont, USA) and consists of an array of 10 parallel  
177 microcapillaries with a mean hydraulic diameter of  $206 \pm 12.6 \mu\text{m}$  (34). The raw MCF strips  
178 are hydrophobic (28), therefore they would require a pressure driven flow for sample loading;  
179 however in this work the MCF strips were made hydrophilic by coating the inside of each  
180 capillary with an hydrogel, poly(vinyl alcohol) (PVOH) (28). In this way the MCF strips  
181 could be filled simply by capillary action ('dip stick' mode). During the coating procedure  
182 100 mL of an aqueous solution of PVOH (MW 13 000–23 000, >98 % hydrolysed from  
183 Sigma-Aldrich, Dorset, UK) with concentration of 5 mg/mL was recirculated through a 6 m

184 long MCF at a flowrate of 50 mL/h for 12-15 hrs using a FPLC P-500 Pharmacia Biotech  
185 (Piscataway, USA) pump and Upchurch flangeless tube fittings (Kinesis, Saint Neots, United  
186 Kingdom). After that, the PVOH coating was crosslinked with glutaraldehyde by manually  
187 filling the MCF strip with a freshly prepared solution of PVOH (5 mg/mL) containing 5 mM  
188 of glutaraldehyde (Sigma-Aldrich, UK) and 5 mM HCl (Sigma-Aldrich, UK). The solution  
189 was kept inside the strips for 2 hours at 37 °C, after which the MCF strips were manually  
190 washed and dried with air using a 50 mL syringe (34).

### 191 ***Solid form screening experiments in the MMicroCryGen platform***

192 For each experiment different solutions were prepared and loaded in the MMicroCryGen  
193 platform using the same procedure. The central Perspex cover was positioned on the  
194 aluminium frame and secured with four screws, then 8 hydrophilic or hydrophobic MCF  
195 strips of 70-80 mm length were inserted in the slots. For hydrophilic strips, the frame was  
196 positioned vertically above a 96 wells microplate loaded with clear API solutions and then  
197 lowered in order to fully immerse the tip of each strip in the wells. For hydrophobic strips,  
198 the microcapillaries were aspirated using a multi-syringe aspiration device reported elsewhere  
199 (34). On both cases, after complete filling of the capillaries with solution, the frame was  
200 placed in horizontal position and the lateral aluminium edges were secured with 8 screws (4  
201 at each side), automatically sealing both ends of the microcapillaries. The frame containing  
202 the MCF strips was then placed on the Peltier heat exchanger and the desired temperature or  
203 cooling profile set from the temperature control software. On-line monitoring of the  
204 experiments was performed with a USB Microscope (5.0 Megapixels supplied by MAOZUA,  
205 China). The MMicroCryGen device allows 80 independent parallel crystallization  
206 experiments in one go, this can be easily further expanded by increasing the number of strips.

207 Once crystals were formed within the microcapillaries, the whole frame was removed from  
208 the Peltier unit and the MCF strips were individually analysed for crystal morphology and

209 polymorphism. A Raman microscope DXR 780 nm (Thermo Scientific equipped with  
210 OMNIC 8 software) equipped with a Linkam hot-stage was used to identify the structure of  
211 the crystals produced.

212 For the polymorph screening experiments succinic acid (SA) and ortho-aminobenzoic acid  
213 (OABA) were used as solid compounds. Only deionized water was the solvent for succinic  
214 acid, while mixtures of deionized water and isopropyl alcohol were used for OABA. A  
215 solution of SA in water with concentration of 0.145 g/g solvent was prepared at 50 °C and  
216 loaded in one row of a standard 96-wells microplate before being interfaced with the  
217 MMicroCryGen. The MCF strips were then cooled down to 5.0 °C at a rate of -0.5 °C/min.  
218 For OABA polymorph screening solutions at different concentrations of OABA were  
219 prepared and loaded into the capillaries at 60 °C, before being cooled down to 3.0 °C at a rate  
220 of -1.0 °C/min.

221 Piroxicam in mixtures of deionized water and acetone was used in the hydrate screening  
222 experiments. Four solutions at different concentrations of piroxicam as well as solvent  
223 composition were prepared at 50 °C and loaded in duplicated MCF strips. The temperature  
224 was reduced to 3.0 °C at a rate of -1.0 °C/min.

225 In the co-crystal screening experiments, p-Toluenesulfonamide and triphenylphosphine oxide  
226 were used with acetonitrile as solvent. Two solutions containing both components in specific  
227 stoichiometric ratios were prepared at 50.0 °C, and each loaded into four MCF strips. After  
228 that, the temperature was reduced to 3.0 °C at a rate of -1.0 °C/min.

229 Finally, a set of experiments was conducted in the presence of o-toluic acid (OTA) in order to  
230 determine the effect of a structurally related additive on the crystallization of OABA. Four  
231 different aqueous solutions with concentration of OABA of 0.010 g/g water and different

232 ratios OTA/OABA w/w were prepared at 50 °C and loaded into the MCF strips. After that the  
233 temperature was reduced to 5.0 °C at a rate of -1.0 °C/min.

234 In all experimental sets, the MMicroCryGen was further incubated overnight at 5.0 °C  
235 enabling full growth of crystals upon completion of the cooling stage.

236

## 237 **Results and discussion**

### 238 *Polymorph screening of SA and OABA*

239 SA is known to have two polymorphic forms,  $\alpha$  and  $\beta$ , which are enantiotropically related.  
240 The triclinic  $\alpha$ -form is usually obtained by solid transformation from the  $\beta$ -form at  
241 temperatures above 137 °C while the monoclinic  $\beta$ -form is the polymorph that generally  
242 precipitates from water in various morphologies (29, 30). Microphotographs for SA crystals  
243 nucleated in the MMicroCryGen platform are shown in Figure 3b-3e, whereas Figure 3a  
244 shows plate-like crystals of  $\beta$ -form only nucleated from an aqueous solution of the same  
245 concentration in a 350 mL vessel with overhead stirring (29). Both high aspect ratio needles  
246 and plate-like crystals were observed in the MCF strips. Raman spectroscopy analysis (Figure  
247 4) confirmed the needle SA crystals were of  $\alpha$ -form. The spectra of these crystals were also  
248 compared with those obtained from hot-stage experiments performed in the available Raman  
249 microscope. SA  $\beta$ -form crystals were heated up above the transition temperature of 137 °C  
250 and then quickly cooled down to ambient temperature to allow the formation of the  $\alpha$ -form on  
251 the hot-stage. Crystallisation in the MCF strips resulted in formation of SA crystals in their  $\alpha$ -  
252 form, which is usually not observed in cooling crystallization in aqueous solutions. This is  
253 presumably due to both the reduced volume and the absence of convection and turbulent  
254 mixing in the microfluidic strips of the MMicroCryGen device. Such conditions promote

255 primary over secondary nucleation, allowing the formation of a larger number of possible  
256 crystal structures, which is ideal for polymorph screening.

257

258 The Raman spectra for both polymorphs of SA obtained in the MCF strips are shown in  
259 Figure 4, and compared to the spectrum of an empty microcapillary. FEP-Teflon® has  
260 distinct, clear peaks that can be easily identified and subtracted from the total final spectra;  
261 strong intensity FEP-Teflon® peaks can be found at values of Raman shift of 290, 385, 730,  
262 1225, 1300, 1380  $\text{cm}^{-1}$ . Depending on the objective and the size of the analysed crystals, it is  
263 possible to focus the Raman laser on a single crystal, avoiding the signal from the MCF strip.  
264 Both hydrophilic and hydrophobic capillaries were tested and no differences were observed  
265 in respect to SA polymorph formation. In fact, both structures were always obtained,  
266 suggesting that the chemistry of the capillary's inner surface did not have a templating effect  
267 on the nucleation of this compound.

268

269 Polymorph screening in different solvent mixtures was performed with OABA. The solvent  
270 compositions and OABA concentrations for each MCF strip are summarised in Table 1. In  
271 contrast to OABA crystallisation experiments previously conducted at larger scale, where  
272 only form I and II could be precipitated in water/IPA mixtures (31), all three known  
273 polymorphs of OABA were obtained in the capillaries, similarly to what was observed with  
274 SA. It can also be noted that, due to the slower kinetics of nucleation in small volumes, some  
275 capillaries did not show any visible crystals in the time scale used for experiments (around  
276 18-24 hrs).

277

278

**Table 1: Experimental conditions and results for polymorph screening of OABA.**

<b>MCF strip number</b>	<b>Solvent composition (% of IPA in water, w/w)</b>	<b>OABA concentration (g/g solvent)</b>	<b>Crystals nucleated in each MCF strip</b>
1	0	0.010	0
2	2%	0.010	1 (form I)
3	5%	0.010	0
4	10%	0.015	0
5	15%	0.020	2 (form II)
6	20%	0.030	2 (form II) 5 (form III)
7	25%	0.055	4 (form II) 2 (form III)
8	30%	0.080	1 (form II) 3 (form III)

279

280 The MMicroCryGen device allowed to identify all the three known forms of OABA from a  
 281 small amount of material, demonstrating the advantage of using this novel methodology for  
 282 polymorph screening. The area in the Raman spectrum that unequivocally identifies the three  
 283 OABA polymorphs is between 1500 and 1700  $\text{cm}^{-1}$  (Figure 5). Form I presents a peak at  
 284 1665  $\text{cm}^{-1}$  and a doublet at 1600  $\text{cm}^{-1}$ , form II has a strong peak at 1565  $\text{cm}^{-1}$  and form III  
 285 presents the same peak but shifted to 1560  $\text{cm}^{-1}$ . Finally, form III is characterized by a strong  
 286 peak at 1610  $\text{cm}^{-1}$ , which is not present in form I and it is weaker in form II.

287

288 The polymorphs screening experiments performed in the MMicroCryGen platform show the  
 289 advantage of using small volumes in the absence of mixing for the discovery of new crystal  
 290 structure.

291 ***Hydrate detection for Piroxicam***

292 Piroxicam was crystallized in different mixtures of acetone and water in order to identify the  
293 possible polymorphs and confirm the presence of hydrate forms. Table 2 shows the  
294 experimental conditions and the different polymorphs identified by Raman spectroscopy, all  
295 known polymorphs and the hydrate form (35-37) were detected in the microcapillaries.  
296 Microscopic images of the two polymorphs are shown in Figure 6b, with the thin needles  
297 characteristic of form II clearly distinguishable from the prismatic form I crystals. The  
298 monohydrate form of piroxicam was obtained in all solutions containing water. These  
299 crystals have a characteristic bright yellow colour as shown in Figure 6a.

300

301

**Table 2: Experimental conditions and results for polymorph screening of piroxicam.**

<b>MCF strip number</b>	<b>Solvent composition (% w/w)</b>	<b>Concentration (g/g solvent)</b>	<b>Crystals nucleated in each MCF strip</b>
1-2	100% acetone	0.040	Anhydrous form I and form II
3-4	5% water in acetone	0.035	Anhydrous form II (needles) and monohydrate (prism)
5-6	20% water in acetone	0.013	Piroxicam monohydrate
7-8	30% water in acetone	0.009	Piroxicam monohydrate

302

303 Raman spectroscopy was also used to distinguish among the polymorphs and the  
304 monohydrate form of piroxicam within the MCF strips. Figure 6c shows the region between  
305 1500 and 1700  $\text{cm}^{-1}$ , where the three forms can be identified without interference from the  
306 FEP-Teflon®. The monohydrate form is characterized by a single strong peak at 1590  $\text{cm}^{-1}$ ,



307 whereas form I has a high intensity peak at  $1520\text{ cm}^{-1}$  and finally, form II is the only  
308 polymorph with a peak at  $1540\text{ cm}^{-1}$ .

309

310 In the case of piroxicam, the MMicroCryGen enabled simultaneous identification of the two  
311 known polymorphs and the hydrate form in a single experiment with four different solutions  
312 of piroxicam in acetone and water mixtures.

### 313 *Screening for co-crystals*

314 A further set of experiments was carried out aiming to demonstrate the application of the  
315 MMicroCryGen device to identify co-crystal structures, using p-Toluenesulfonamide (p-  
316 TSA) and Triphenylphosphine oxide (TPPO) as model compounds.

317

318 **Table 3: Experimental conditions and structures obtained during the screening of TSA/TPPO co-crystals.**

<b>Solvent composition</b> <b>(% w/w)</b>	<b>Concentration</b> <b>p-TSA</b> <b>(g/g solvent)</b>	<b>Concentration</b> <b>TPPO</b> <b>(g/g solvent)</b>	<b>Crystals nucleated in each MCF</b> <b>strip</b>
100% acetonitrile	0.02987	0.01492	3:2 co-crystal form
100 % acetonitrile	0.01154	0.01489	1:1 co-crystal form

319

320 The two co-crystals known for those chemicals, with molecular ratio p-TSA/TPPO 3:2 and  
321 1:1 (33), were quickly and successfully identified in a single experiment in the  
322 MMicroCryGen device, as confirmed by Raman spectroscopy according to data available  
323 from literature (33). Experimental conditions are described in Table 3, whereas the Raman  
324 spectra of the two co-crystal forms obtained are shown in Figure 7. The Raman spectra for

325 pure p-TSA and TPPO were compared to data available in literature (33, 38), confirming the  
326 formation of two co-crystal forms. The characteristic regions of the Raman spectrum for the  
327 unequivocal identification of the two co-crystal forms are shown in Figure 7. Characteristic  
328 peaks for the 1:1 co-crystal are located at 317, 460, 507, 934 and 1151  $\text{cm}^{-1}$ , whereas the 3:2  
329 co-crystal is characterized by specific peaks at 310, 915 and 1149  $\text{cm}^{-1}$ (Figure 7).

330 These experimental demonstrate the use of ‘dip stick’ microcapillaries for discovery of new  
331 co-crystal structures. Furthermore, the use of the MMicroCryGen platform allowed the  
332 identification of such co-crystal forms running a single experiment, with the use of limited  
333 amount of chemicals as well as solvents.

334

### 335 *Screening of the effect of additives on polymorphism*

336 Additives can have an effect on the polymorphic outcome of crystallization processes. These  
337 additives can act by inhibiting nucleation or growth of a certain polymorph of the main  
338 crystallizing compound, therefore stabilizing a different form. They can also stereo-  
339 selectively bind to specific surfaces of the targeted crystal nuclei, inhibiting their growth and  
340 therefore modifying the morphology of the crystals (32). The MMicroCryGen device was  
341 used to determine the effect of a structurally related additive (o-toluic acid, OTA) on the  
342 polymorphic outcome of OABA. Experiments at larger scale conducted with this compound  
343 and a similar molecule (benzoic acid) showed that a structurally related additive promoted  
344 nucleation of OABA form III, which can normally be obtained only by sublimation or  
345 polymorphic transformation at temperatures higher than the transition one (around 60 °C)  
346 (32). Four aqueous solutions at different ratios OTA/OABA were loaded into the MCF strips  
347 before starting the cooling profile. Table 4 shows the polymorphs detected in the capillaries.

348

349 **Table 4: Polymorphic outcome of cooling crystallization of OABA in the presence of the structurally related**  
350 **molecule OTA.**

<b>MCF strips number</b>	<b>Ratio OTA/OABA w/w</b>	<b>OABA polymorphs identified in MCF</b>
1-2	0	Form I and II
3-4	5%	Form I, Form II, Form III
5-6	10%	Form III
7-8	15%	Form III

351

352

353 Similarly to previously reported observations at larger scale experiments with benzoic acid  
354 (32), the addition of a structurally related additive promotes the formation of OABA form III  
355 in water. In fact, only form I and II were nucleated in water in the absence of additive,  
356 whereas preferential nucleation of only form III could be observed at increasing  
357 concentrations of OTA. This indicates that, similarly to benzoic acid, OTA has an effect on  
358 the polymorphic outcome of OABA crystals generated via cooling. Crystallization  
359 experiments in the MMicroCryGen platform allowed easier determination of the effect of a  
360 structurally related additive on the crystallization of OABA using a considerably lower  
361 amount of solvent and materials compared to experiments conducted at larger scale (32).

## 362 **Conclusions**

363 The presented microfluidic MMicroCryGen crystallization device represents a valuable novel  
364 solution for polymorph and co-crystal screening of small molecules, requiring a smaller  
365 amount of compound and solvents and considerably fewer and cheaper fluidics and electronic  
366 instrumentation compared to standard microfluidic techniques, as well as larger scale  
367 equipment. The device and methodology proposed has the ability of enabling up to 80  
368 parallel crystallization experiments without any pipetting or complex fluid handling, which

369 could be particularly useful during the early stages of drug development when only a small  
370 amount of material is available, and for the study of particularly toxic, genotoxic or  
371 carcinogenic APIs. In this paper the MMicroCryGen platform was validated for solid form  
372 screening of SA, OABA, Piroxicam and the TSA/TPPO system. All known polymorphs,  
373 hydrates and co-crystals of the systems studied were identified with a reduced number of  
374 experiments and using very small amounts of material. The MMicroCryGen platform could  
375 also be used for more complex experiments including the study of the effect of additives on  
376 crystal forms resulting from cooling crystallization.

377

### 378 **Conflicts of interest**

379 There are no conflicts of interest to declare.

380

### 381 **Acknowledgments**

382 This work has been funded through the European Research Council grant no. [280106-  
383 CrySys]. The authors would like to thank Patrick Hester at Lamina Dielectrics Ltd for  
384 providing the MCF material, Antony Eyre at Loughborough University for assistance in  
385 designing and manufacturing the MMicroCryGen device and Dr Ana Isabel Barbosa for  
386 assistance with the MCF experiments and fluid aspiration procedure on hydrophobic MCF  
387 strips.

388

### 389 **References**

390 1. Bernstein J. Polymorphism - A perspective. Cryst Growth Des.  
391 2011;11(Perspective):632–50.

- 392 2. Bernstein J. Polymorphism in molecular crystals. First. Oxford Science Publication;  
393 2002.
- 394 3. Brittain HG. Polymorphism in pharmaceutical solids. Second. CRC Press Taylor a&  
395 Francis Group; 2009.
- 396 4. Lee EH. A practical guide to pharmaceutical polymorph screening & selection. Asian  
397 J Pharm Sci. 2014;9(4):163–75.
- 398 5. Brittain HG. Vibrational studies of cocrystals and salts. 1. The benzamide-Benzoic  
399 acid system. Cryst Growth Des. 2009;9(5):2492–9.
- 400 6. Storey R, Docherty R, Higginson P, Dallman C, Gilmore C, Barr G, et al. Automation  
401 of solid form screening procedures in the pharmaceutical industry - How to avoid the  
402 bottlenecks. Crystallogr Rev. 2004;10(1):45–56.
- 403 7. Lu J, Litster JD, Nagy ZK. Nucleation Studies of Active Pharmaceutical Ingredients  
404 in an Air-Segmented Microfluidic Drop-Based Crystallizer. Cryst Growth Des.  
405 2015;15(8):3645–51.
- 406 8. Ildefonso M, Revalor E, Punniam P, Salmon JB, Candoni N, Veessler S. Nucleation  
407 and polymorphism explored via an easy-to-use microfluidic tool. J Cryst Growth.  
408 2012;342(1):9–12.
- 409 9. Chen ZP, Li LM, Jin JW, Nordon A, Littlejohn D, Yang J, et al. Quantitative analysis  
410 of powder mixtures by Raman spectrometry: the influence of particle size and its correction.  
411 Anal Chem. 2012;84:4088–94.
- 412 10. Vitry Y, Teychené S, Charton S, Lamadie F, Biscans B. Investigation of a  
413 microfluidic approach to study very high nucleation rates involved in precipitation processes.  
414 Chem Eng Sci. 2015;133:54–61.
- 415 11. Teychené S, Biscans B. Crystal nucleation in a droplet based microfluidic crystallizer.  
416 Chem Eng Sci. 2012;77:242–8.
- 417 12. Thorson MR, Goyal S, Gong Y, Zhang GGZ, Kenis PJ a. Microfluidic approach to  
418 polymorph screening through antisolvent crystallization. CrystEngComm. 2012;14(7):2404.

- 419 13. Goyal S, Economou A, Papadopoulos T, Horstman EM, Zhang GGZ, Gong Y, et al.  
420 Solvent Compatible Microfluidic Platforms for Pharmaceutical Solid Form Screening. RSC  
421 Adv. 2016;13286–96.
- 422 14. Horstman EM, Goyal S, Pawate A, Lee G, Zhang GGZ, Gong Y, et al. Crystallization  
423 optimization of pharmaceutical solid forms with X-ray compatible microfluidic platforms.  
424 Cryst Growth Des. 2015;15(3):1201–9.
- 425 15. Goyal S, Thorson MR, Zhang GGZ, Gong Y, Kenis PJ a. Microfluidic approach to  
426 cocrystal screening of pharmaceutical parent compounds. Cryst Growth Des.  
427 2012;12(12):6023–34.
- 428 16. Shi H, Xiao Y, Ferguson S, Huang X, Wang N, Hao H. Progress of crystallization in  
429 microfluidic devices. Lab Chip. 2017;17(13):2167–85.
- 430 17. Chen K, Goh L, He G, Kenis PJA, Zukoski III CF, Braatz RD. Identification of  
431 nucleation rates in droplet-based microfluidic systems. Chem Eng Sci. 2012, 77:235-241.
- 432 18. Goh L, Chen K, Bhamidi V, He G, Kee NCS, Kenis PJA, Zukoski III CF, Braatz RD. A  
433 Stochastic Model for Nucleation Kinetics Determination in Droplet-Based Microfluidic  
434 Systems. Cryst Growth Des. 2010, 10:2515–2521.
- 435 19. Zheng B, Spencer Roach L, Ismagilov RF. Screening of Protein Crystallization  
436 Conditions on a Microfluidic Chip Using Nanoliter-Size Droplets. J Am Chem Soc. 2003,  
437 125(37):11170–11171.
- 438 20. Lee AY, Lee IS, Dette SS, Boerner J, Myerson AS. Crystallization on Confined  
439 Engineered Surfaces: A Method to Control Crystal Size and Generate Different Polymorphs.  
440 J Am Chem Soc. 2005, 127(43): 14982–14983
- 441 21. Wijethunga TK, Baftizadeh F, Stojaković J, Myerson AS, Trout BL. Experimental and  
442 Mechanistic Study of the Heterogeneous Nucleation and Epitaxy of Acetaminophen with  
443 Biocompatible Crystalline Substrates. Cryst Growth Des. 2017, 17(7):3783–3795.
- 444 22. Gerdtz CJ, Stahl GL, Napuli A, Staker B, Abendroth J, Edwards TE, et al.  
445 Nanovolume optimization of protein crystal growth using the microcapillary protein  
446 crystallization system. J Appl Crystallogr. 2010;43(5 PART 1):1078–83.
- 447 23. Zheng B, Tice JD, Roach LS, Ismagilov RF. A droplet-based, composite PDMS/glass  
448 capillary microfluidic system for evaluating protein crystallization conditions by microbatch

449 and vapor-diffusion methods with on-chip X-ray diffraction. *Angew Chemie - Int Ed.*  
450 2004;43(19):2508–11.

451 24. Ji B, Cusack M, Freer A, Dobson PS, Gadegaard N, Yin H. Control of crystal  
452 polymorph in microfluidics using molluscan 28 kDa Ca<sup>2+</sup>-binding protein. *Integr Biol.*  
453 2010;2(10):528.

454 25. Barbosa AI, Gehlot P, Sidapra K, Edwards AD, Reis NM. Portable smartphone  
455 quantitation of prostate specific antigen (PSA) in a fluoropolymer microfluidic device.  
456 *Biosens Bioelectron.* 2015;70:5–14.

457 26. Barbosa AI, Reis NM. A critical insight into the development pipeline of microfluidic  
458 immunoassay devices for sensitive quantitation of protein biomarkers at point-of-care.  
459 *Analyst.* 2017; 142:858-882.

460 27. Reis NM, Li Puma G. A novel microfluidic approach for extremely fast and efficient  
461 photochemical transformations in fluoropolymer microcapillary films. *Chem Commun.*  
462 2015;51(40):8414–7.

463 28. Reis NM, Pivetal J, Loo-Zazueta AL, Barros J, Edwards AD. Lab on a Stick: Multi-  
464 Analyte Cellular Assays in a Microfluidic Dipstick. *Lab Chip.* 2016;16:2891–9.

465 29. Klapwijk AR, Simone E, Nagy ZK, Wilson CC. Tuning Crystal Morphology of  
466 Succinic Acid Using a Polymer Additive. *Cryst Growth Des.* 2016;6(8):4349–4359.

467 30. Simone E, Klapwijk AR, Wilson CC, Nagy ZK. Investigation of the evolution of  
468 crystal size and shape during temperature cycling and in the presence of a polymeric additive  
469 using combined Process Analytical Technologies. *Cryst Growth Des.* 2017; 17(4):1695–  
470 1706.

471 31. Simone E, Nagy ZK. A link between the ATR-UV/Vis and Raman spectra of  
472 zwitterionic solutions and the polymorphic outcome in cooling crystallization.  
473 *CrystEngComm.* 2015;17:6538–47.

474 32. Simone E, Steele G, Nagy ZK. Tailoring crystal shape and polymorphism using  
475 combinations of solvents and a structurally related additive. *CrystEngComm.* 2015;17:9370–  
476 9.

477 33. Powell K a., Croker DM, Rielly CD, Nagy ZK. PAT-based design of agrochemical  
478 co-crystallization processes: A case-study for the selective crystallization of 1:1 and 3:2 co-

479 crystals of p-toluenesulfonamide/triphenylphosphine oxide. *Chem Eng Sci.* 2016;152:95–  
480 108.

481 34. Reis NM, Pivetal J, Loo-Zazueta AL, Barros J, Edwards AD. Lab on a Stick: Multi-  
482 Analyte Cellular Assays in a Microfluidic Dipstick. *Lab Chip.* 2016;16:2891–9.

483 35. Liu G, Hansen TB, Qu H, Yang M, Pajander JP, Rantanen J, et al. Crystallization of  
484 Piroxicam Solid Forms and the Effects of Additives. *Chem Eng Technol.* 2014;37(8):1297–  
485 304.

486 36. Hansen TB, Qu H. Formation of Piroxicam Polymorphism in Solution Crystallization:  
487 Effect and Interplay of Operation Parameters. *Cryst Growth Des.* 2015;15(9):4694–700.

488 37. Simone E, Othman R, Vladislavljević G, Nagy Z. Preventing Crystal Agglomeration  
489 of Pharmaceutical Crystals Using Temperature Cycling and a Novel Membrane  
490 Crystallization Procedure for Seed Crystal Generation. *Pharmaceutics.* 2018;10(1):17.

491 38. Croker DM, Davey RJ, Rasmuson ÅC, Seaton CC. Nucleation in the p-  
492 toluenesulfonamide/triphenylphosphine oxide co-crystal system. *Cryst Growth Des.*  
493 2013;13(8):3754–62.

494



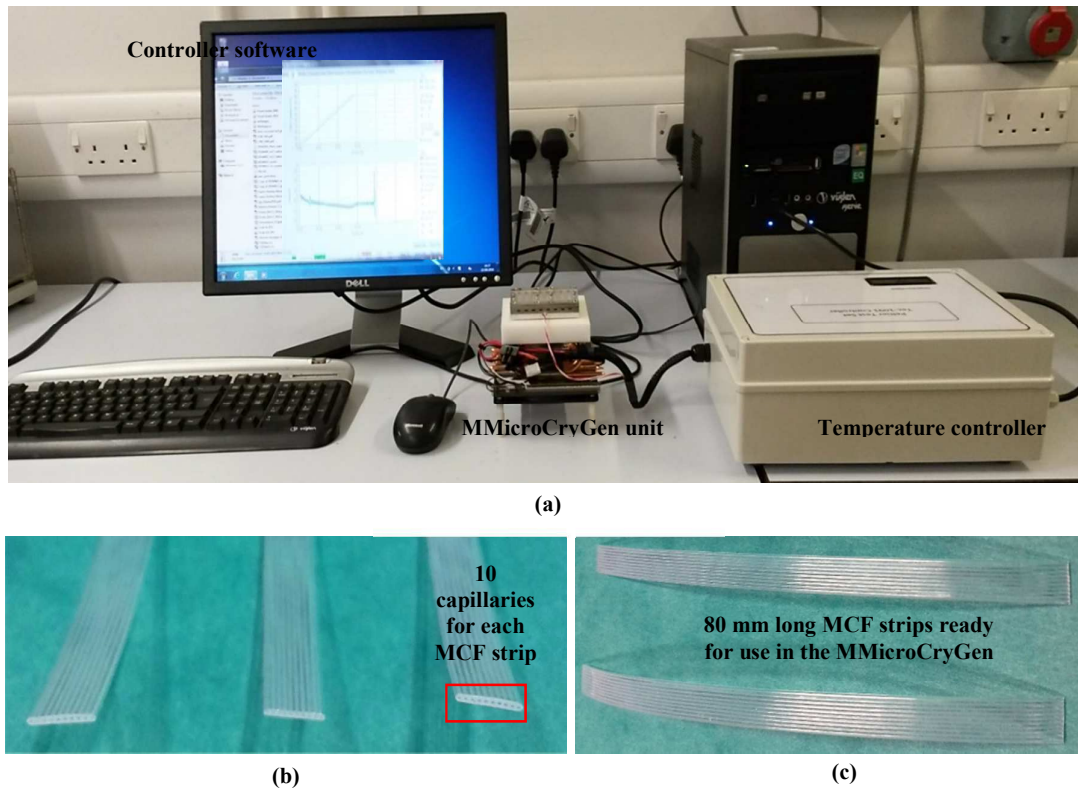


**Figure 1: (a) Photographs of the MMicroCryGen unit with temperature controller for remote temperature setting; (b-c) Photographs of the MCF strips and detail of the 10 internal capillaries**

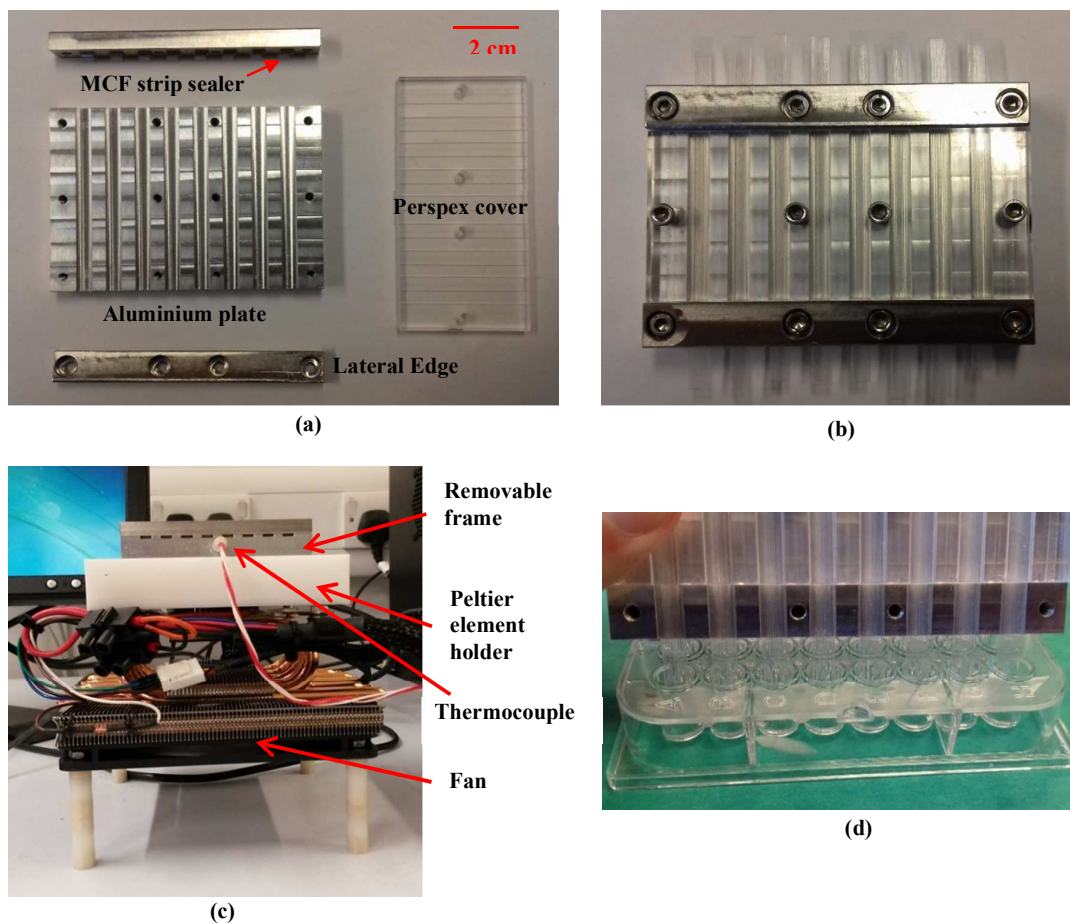


**Figure 2:** (a) Photograph showing the four elements of the removable frame of the MMicroCryGen platform; (b) Assembled frame; (c) Removable frame positioned on the Peltier element holder and fan; (d) Solutions loading procedure for hydrophilic capillaries.

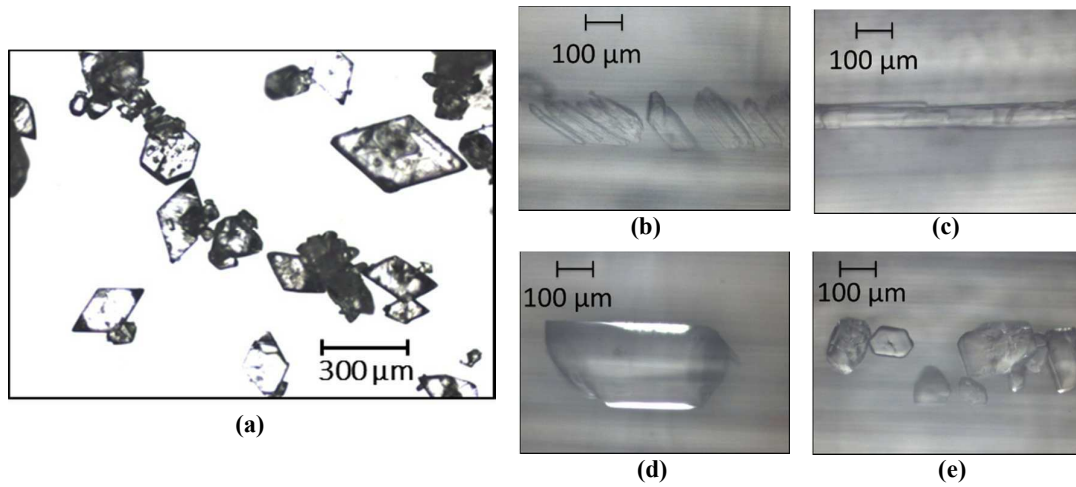


**Figure 3:** (a) Microscopic image of  $\beta$  SA crystals obtained from water in a 350 mL stirred vessel; (b), (c) crystals of  $\alpha$  SA inside an MCF strip; (d), (e) crystals of  $\beta$  SA inside an MCF strip.

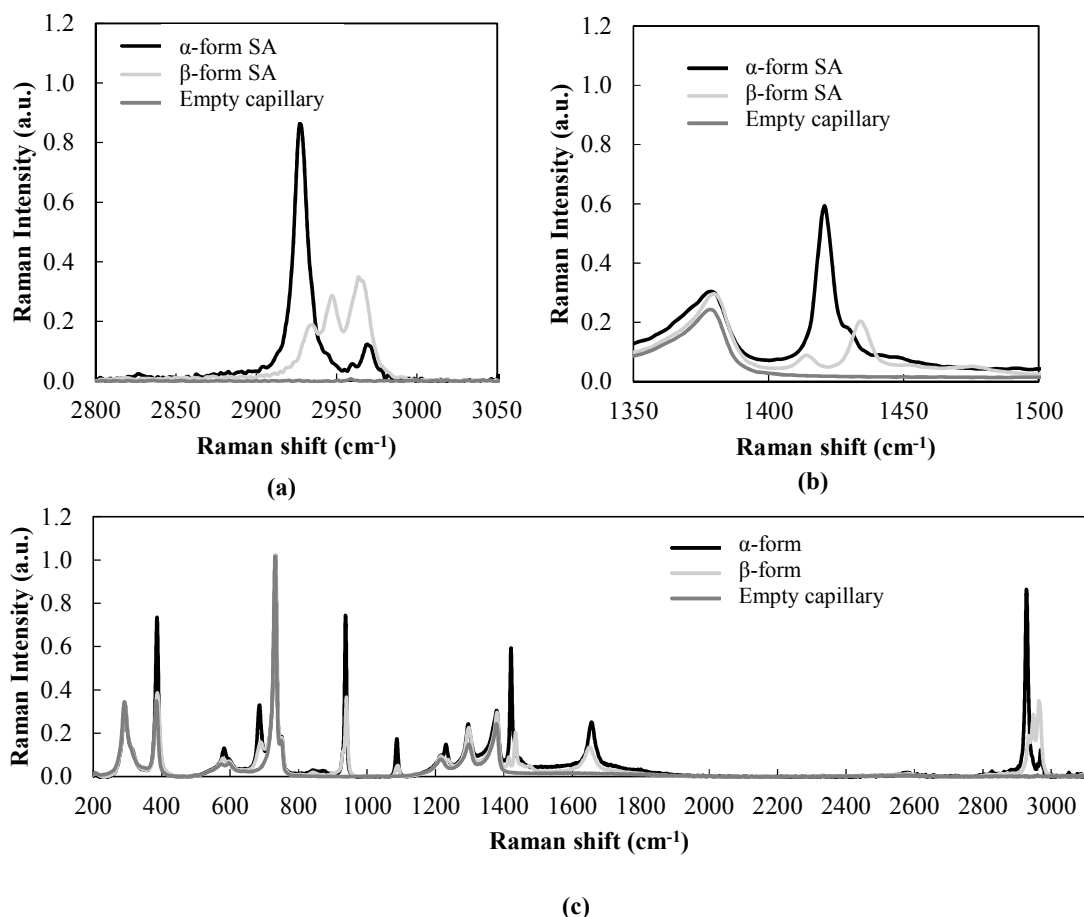


Figure 4: Raman spectra of the two polymorphs of SA inside an MCF strip and an empty capillary of MCF strip. Region (a) 2800- 3050 cm<sup>-1</sup>; (b) 1350-1500 cm<sup>-1</sup> and (c) full spectrum.

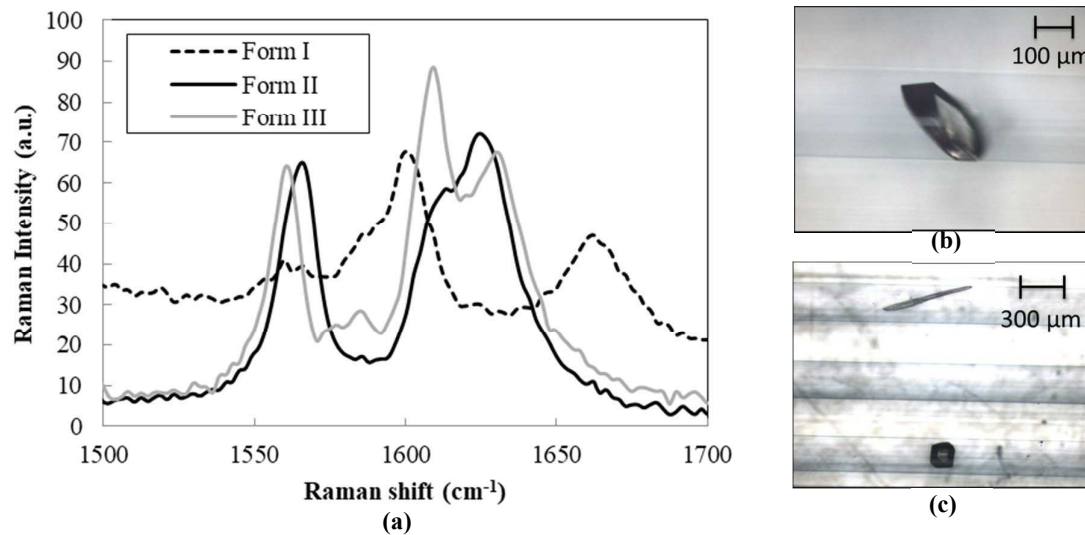
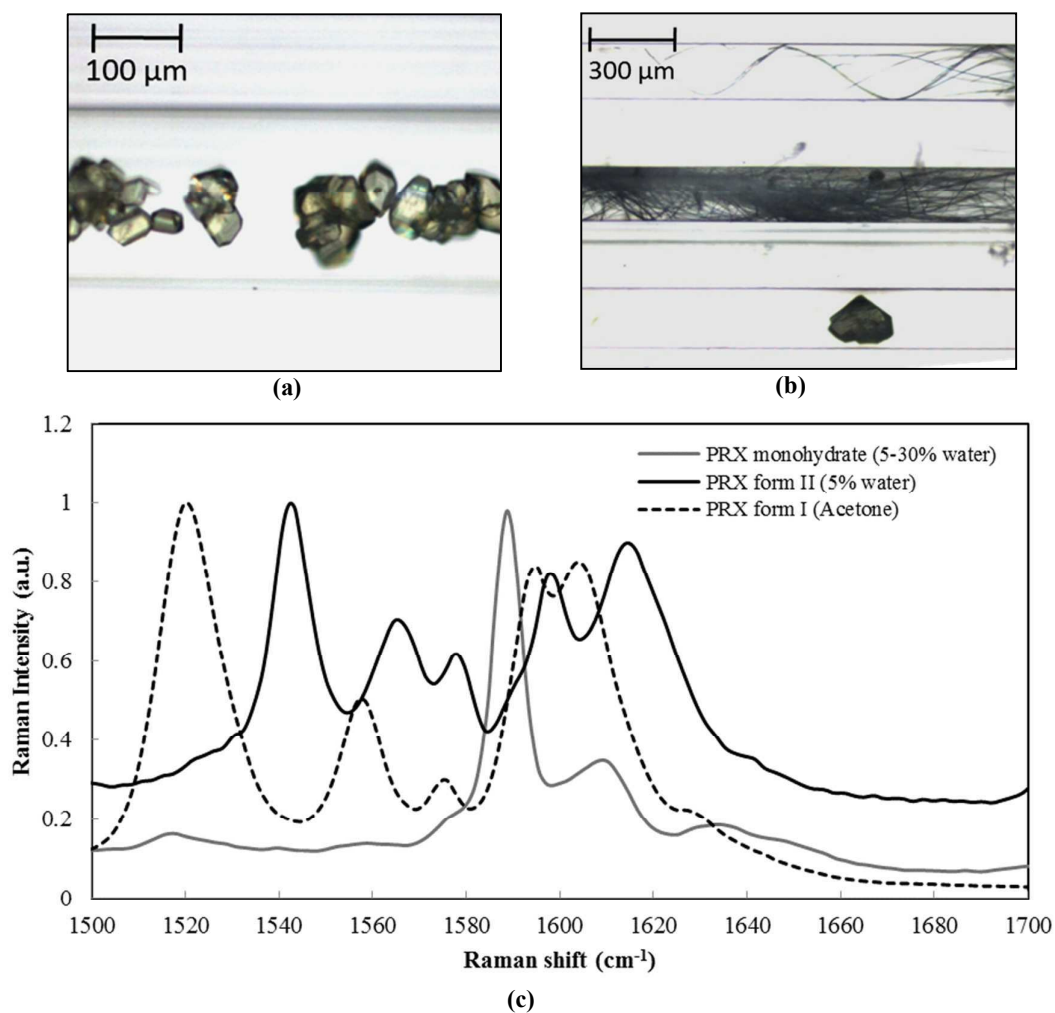


Figure 5: (a) Raman spectra of the different polymorphs of OABA identified in the capillaries (b) Crystal of form III, (c) Crystals of form III on the top capillary and form II on the bottom one.



**Figure 6:** (a) Piroxicam hydrate crystals nucleated from a solution of 30% water in acetone w/w, (b) crystals of Piroxicam anhydrous form II (needles) and monohydrate (prism) nucleated in a solution of 5% water in acetone w/w; (3) Raman spectra of form I, form II and piroxicam monohydrate.

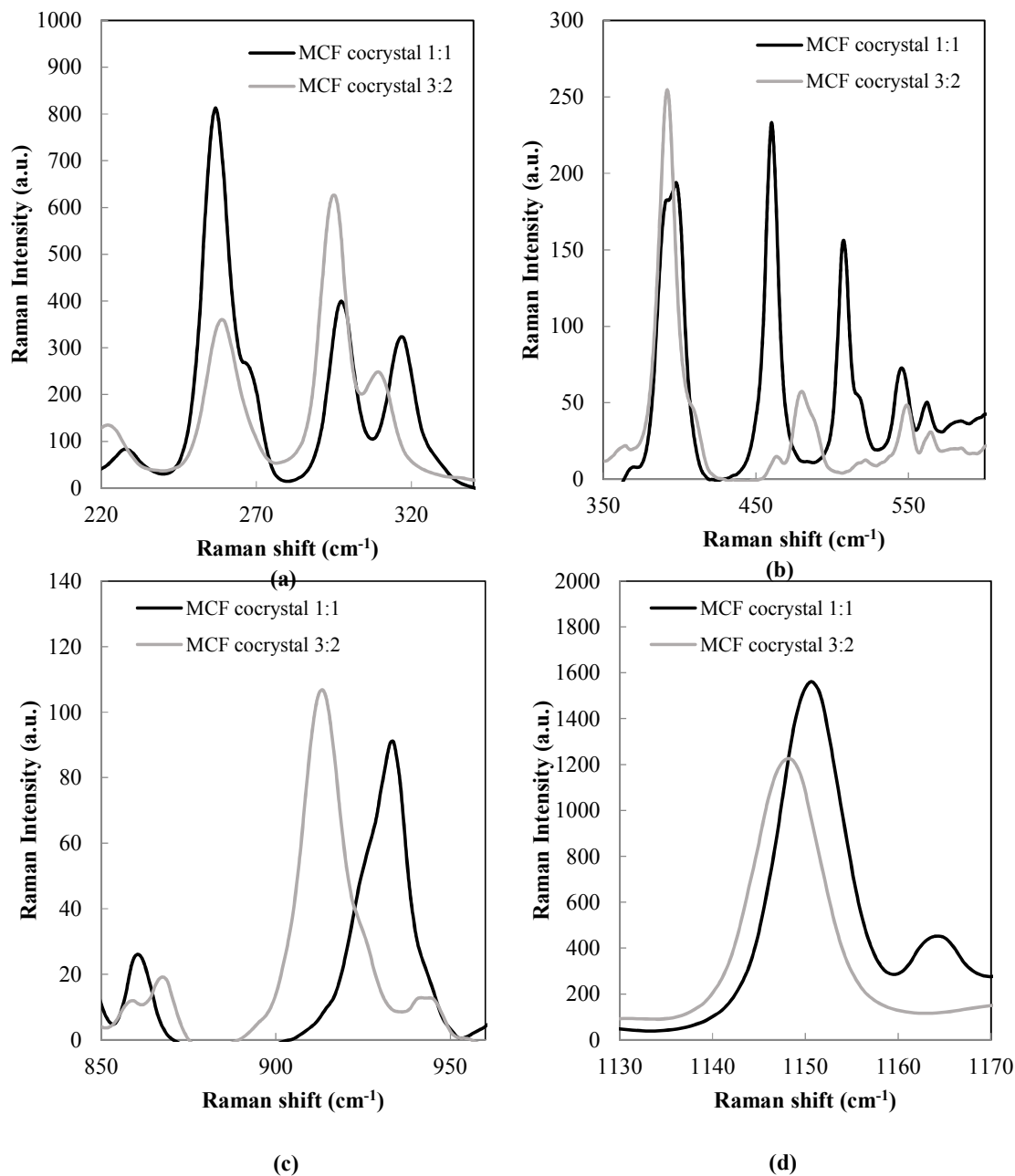


Figure 7: Raman spectra of the different forms of p-TSA/TPPO co-crystals identified in the capillaries. Regions between (a) 220–330 cm<sup>-1</sup>; (b) 350–560 cm<sup>-1</sup>; (c) 850–960 cm<sup>-1</sup> and (d) 1100–1250 cm<sup>-1</sup>.

The MMicroCryGen allows single crystal generation and screening using 200  $\mu\text{L}$  of solvent and without complex fluid handling ('dipstick' mode).

### MMicroCryGen

